Amsterdam '14

We E102 13

AVA Attributes for Lithology and Fluid Discrimination Based on a Quadratic Form of Zoeppritzs Equations

R. Negrete Cadena* (Pemex/Imperial College London), Y. Wang (Imperial College London) & J. Morgan (Imperial College London)

SUMMARY

In AVA analyses, simplified linear approximations to Zoeppritz's equations are often used, but do not always work well. Here, we investigate the use of an AVA attribute derived from a quadratic approximation to Zoeppritz's equations, hereafter referred to as QAF (Quadratic AVA Factor). We have evaluated its performance trhough applying it to a field example and we found that, when our QAF attribute is combined with a fluid content attribute (Quadratic Fluid Factor QFF), it performs well in comparison to approaches that utilize a linear approximation. The attribute QAF is able to detect major lithological changes and to distinguish between high and low impedance sands. The AVA indicator QFF is able to discriminate between brine-filled, gas-filled or light oil-filled sands. Based on these results we conclude that the QFF indicator is a promising new tool for reservoir characterization.

Introduction

The analysis of the amplitude variation with offset (AVO) or the angle of incidence (AVA) is an effective tool in the identification of fluid content and lithological changes within hydrocarbon reservoirs. AVA analysis is based on the energy partitioning principle, which depends on the variation of three elastic properties across an interface: P-wave velocity (V_P), S-wave velocity (V_S) and density (ρ). AVA analyses use Zoeppritz's equations or their approximations, which describe the transformation of a seismic wave reflected from an interface of interest (i.e. a potential hydrocarbon bearing layer).

Zoeppritz's equations describe the reflection and transmission amplitudes accurately (Aki and Richards, 1980). The complexity of these equations, however, means that inverting observed amplitudes to obtain physical properties is non-trivial. Many authors (Bortfeld, 1962; Shuey, 1985; Fatti et al., 1994; Verm and Hilterman, 1995; Gray et al., 1999) have developed a number of linear approximations in order to obtain relationships between seismic attributes and reservoirs properties. Linear approximations are utilized to obtain a range of AVO/AVA attributes: P-impedance reflectivity (R_P) Intercept (I) and Gradient (G) (Shuey, 1985), P- and S-velocity reflectivities (R_{V_P} and R_{V_S}) (Smith and Gidlow,1987), P- and S-impedance reflectivities (R_P and R_S) (Fatti *et al.*,1994) and Lambda reflectivity ($\Delta\lambda/\lambda$) and Mu reflectivity ($\Delta\mu/\mu$) (Gray *et al.*, 1999).

The main objective behind these approaches is to obtain attributes and hydrocarbon indicators which allows effective discrimination between potential hydrocarbon bearing layers and the background. One of the most commonly used AVA indicators is the product of the Intercept and Gradient obtained by using Shuey's approximation. According to Castagna *et al*, 1994, $I \times G$ product is a good indicator of bright spots, themselves a direct hydrocarbon indicator.

AVA attributes have been used by the petroleum industry to identify plays within the Gulf of Mexico but it has been noted that some of the inverted attributes derived from linear approximations have been inaccurate and misleading (Adamick *et al.*, 1994). This may well be because the linearized inversion applied in these cases inverts for only two elastic parameters and assumes that the S- to P-wave velocity ratio is known (Wang, 1993). Such a constraint will lead to inaccuracies if these conditions are not met.

Quadratic approximations to Zoeppritz's equations provide a more accurate solution than linear ones and thus might be expected to be useful in AVA analyses. We have conducted a suite of synthetic tests designed to evaluate the use of a quadratic approximation in both the classification of sands and as an indicator of fluid content. Here, we show how they perform 2D synthetic AVA indicators.

Quadratic approximation to Zoeppritz's equations

Wang (1999) derived quadratic expressions (Equation 1) for the P-wave reflection and transmission coefficients for different incidence angles (θ) as a function of three elastic contrasts at an interface: relative P-wave velocity contrast, $\Delta\alpha/\alpha$, relative S-wave velocity contrast $\Delta\beta/\beta$ and the ratio of P-wave and S-wave velocities β/α, which is not assumed to be a constant:

$$\mathrm{R}_{pp} = A\frac{\Delta\alpha}{\alpha} + B\frac{\Delta\beta}{\beta} + C\left(\frac{1}{4}\frac{\Delta\alpha}{\alpha} + 2\frac{\Delta\beta}{\beta}\right)^2, \quad (1)$$

where

$$A = \frac{5}{8} + \frac{1}{2}\tan^2\theta - \frac{1}{2}\left(\frac{\beta}{\alpha}\right)^2\sin^2\theta, \quad B = -4\left(\frac{\beta}{\alpha}\right)^2\sin^2\theta, \quad C = \left(\frac{\beta}{\alpha}\right)^3\cos\theta\sin^2\theta$$

and θ is the incident angle. The third term in Equation (1) is in the form of a quadratic binomial. We define this quadratic binomial as the Quadratic AVA Factor (*QAF*):

$$QAF = C\left(\frac{1}{4}\frac{\Delta\alpha}{\alpha} + 2\frac{\Delta\beta}{\beta}\right)^2 \quad (2)$$

We can see that, in this term, S-wave velocity contrasts are doubled while P-wave velocity contrasts are reduced by a quarter. Therefore, we suggest that QAF values will be higher for major changes in lithology (e.g. interfaces between shale and sand layers) since these are expected to more strongly affect S-wave velocities.

Synthetic tests

We have constructed a synthetic 2D velocity model to investigate the performance of AVA attributes and AVA indicators. The velocity model contains an anticlinal structure that has similarities with real reservoirs in the Gulf of Mexico. The model was built using a number of geological interpretations of seismic horizons in regional seismic reflection data. The P-wave velocity model (Figure 1a) was created using high-density interval velocity information (Figure 1b), which was calibrated with the sonic log from a light oil producer well. P-wave velocity functions (Figure 1b) extracted along the model show a light oil sand layer between 4000 and 4500 meters, which approximately corresponds with reservoir 2. S-wave velocity was determined using Krief's equation (Krief *et al*., 1990) for each of the vertical functions inside the reservoir and by using Castagna's equation (Castagna *et al*., 1985) for the functions outside. Gardner's relationship (Gardner *et al.*, 1974) was used to predict density. The P-wave velocity, S-wave velocity and density models were then used to calculate the attributes shown in Figures 2-4.

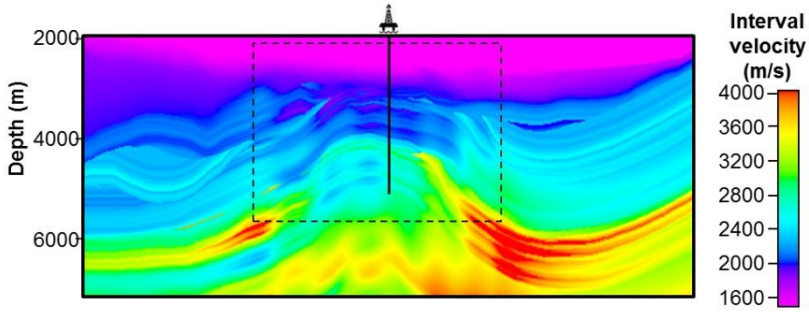

(a)

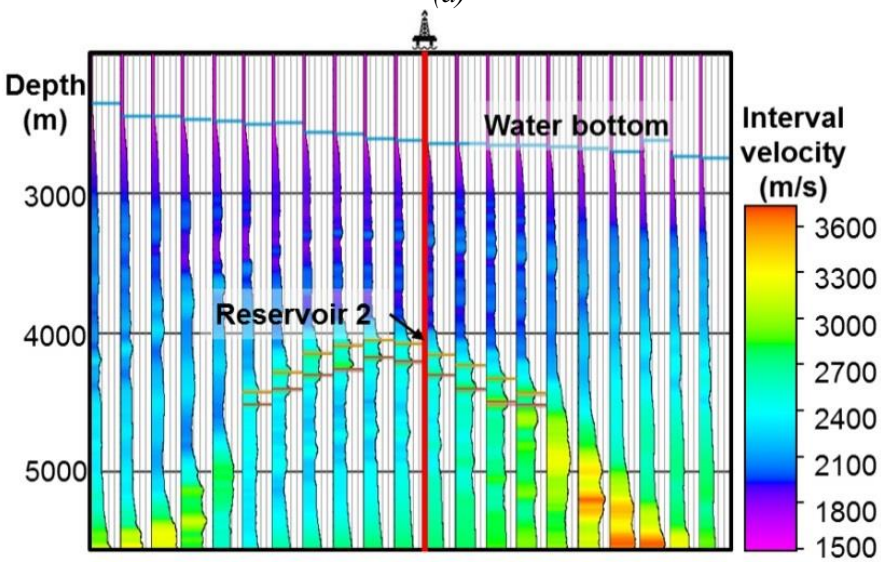

(b)

Figure 1 *(a) Interval velocity model for the anticline structure of the reservoir. The dashed square shows the area of interest. (b) Vertical functions extracted from the interval velocity model inside the area of interest. The top and base of the reservoir are highlighted by light brown and dark brown lines between 4000m and 4500m.*

We calculated a number of AVA attributes: Intercept (I) or R_P, Gradient (G), R_S, $\lambda\rho$, $\mu\rho$, Fluid Factor *(FF)* (Fatti et al, 1994) and *QAF*. Furthermore we obtained a range of AVA indicators in order to evaluate them effectiveness for hydrocarbon-bearing detection. $[R_P - R_S]$ and $[I \times G]$ values are shown in Figure 2a and 2b respectively. According to Castagna et al. (1994) we expect negative values of $[R_P - R_S]$ and positive values of $[I \times G]$ to occur at the top of the reservoir, and for this particular example the $[I \times G]$ indicator appears to be more successful in identifying the reservoir between 4000-4500 m. As mentioned in the previous section, higher values of *QAF* can be indicative of reservoir sand.

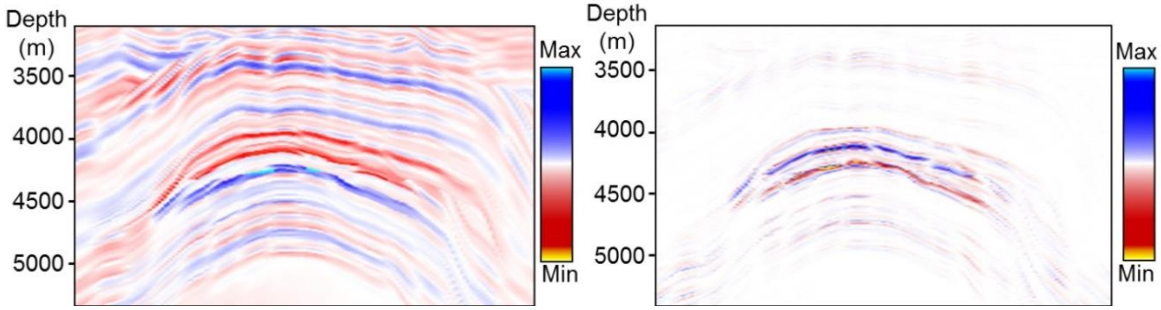

(a) *(b)*

Figure 2 *$[R_P - R_S]$ (a) and $[I \times G]$ (b) AVA indicators. Red and yellow colors indicate lower values and blue colors indicate higher values.*

Figure 3a shows high values of *QAF* not only at the top and base of the reservoir but also in some layers above, which are likely to reflect lithological changes. Therefore *QAF* alone does not provide a clear discrimination between hydrocarbon and water bearing reservoirs. To address this we have combined an AVA fluid content attribute with *QAF*. In Figure 3b we have plotted *QAF* multiplied by *FF* to obtain a new AVA indicator, hereafter referred Quadratic Fluid Factor (*QFF*). It is clear that, for this example, the *QFF* can detect the top and base of the reservoir, as well as the $[I \times G]$ plot shown in Figure 2b.

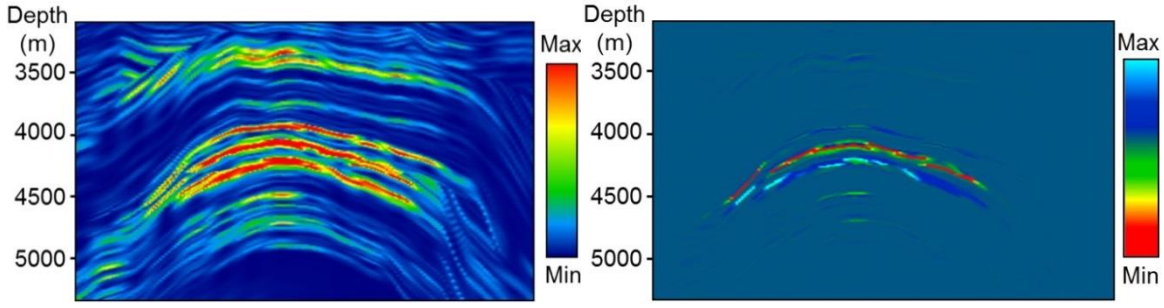

(a) *(b)*

Figure 3 *QAF attribute (a) and QFF indicator (b). Red colors of QAF are related to sand distribution. Red and blue colors of QFF show the top and base of the reservoir respectively.*

Figure 4 shows a more complete set of AVA attributes and AVA indicators extracted at the well position (Figure 1). The *QFF* is able to locate accurately the top (red) and bottom (blue) of this reservoir, and is just as good as the commonly used $I \times G$ or $\lambda\rho\mu\rho$ AVA indicators.

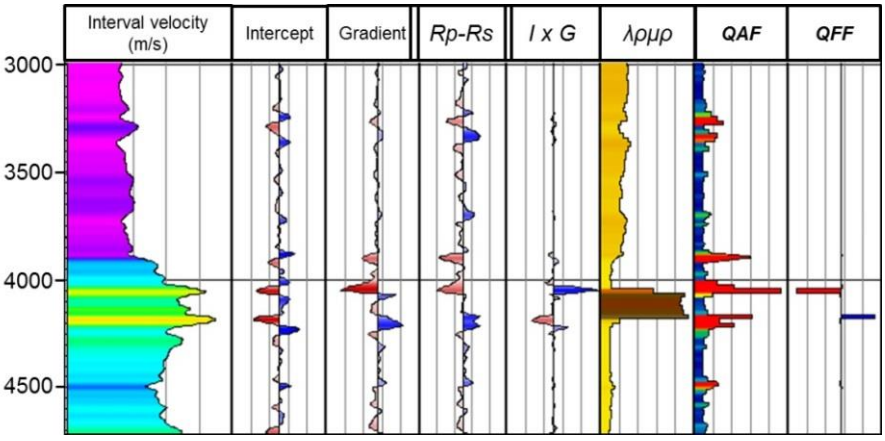

Figure 4 *Vertical functions of interval velocities, AVA attributes (Intercept, Gradient and QAF) and AVA indicators ($[I \times G]$,$[R_P - R_S]$, $\lambda\rho\mu\rho$ and the Quadratic Fluid Factor QFF) extracted along the well location.*

Conclusions

Two new AVA attributes, the Quadratic AVA Factor (*QAF*) and Fluid Quadratic Factor (*QFF*), have been derived from a quadratic approximation to Zoeprittz's equations. In agreement with Wang (1999) we confirm that all our tests indicated that a quadratic approximation is at least as good as a linear approximation of Zoeppritz's equations. We have shown that both *QAF* and *QFF* are useful for reservoir characterization. The *QAF* attribute is sensitive to lithology and could be used as a seismic attribute for the identification and classification of sandstones. For the example shown here, *QFF* was an effective AVA indicator of hydrocarbon-bearing reservoirs. Our results are promising and the next step is to incorporate the quadratic approximation in an AVA inversion. These two new attributes could be developed further through the derivation of new AVA indicators from mathematical operations between the *QAF*, *QFF* and other AVA attributes.

Bibliography: Adamick JH, Skoyles D, DeWildt, J, and Erickson, J, 1994, AVO as an exploration tool: Gulf of Mexico case studies and examples. 64th Annual Internat. Mtg., Soc. Expl. Geophys., Expanded Abstracts, **94**, 1107-1111; **Aki K., and Richards PG**, 1980. Quantitative Seismology, W.H. Freeman and Co., New York; **Castagna JP and Smith SW**, 1994, Comparison of AVO indicators: A modeling study. Geophysics, 59, 1849-1855; **Fatti JL, Smith GC, Vail PJ, Strauss PJ, Levitt PR**, 1994, Detection of gas in sandstone reservoirs using AVO analysis, A 3D seismic case history using the Geostack technique, Geophysics, 59, 1362-1376;**Gray, FD, Goodway, WN and Chen, T**, 1999, Bridging the Gap: Using AVO to detect changes in fundamental elastic constants: 69th Annual Internat. Mtg., Soc. Expl. Geophys., Expanded Abstracts, 852-855; **Goodway, W, Chen, T, and Downton**, J, 1997, Improved AVO fluid detection and lithology discrimination using Lamé petrophysical parameters. Extended Abstracts, Soc. Expl., Geophys., 67th Annual International Meeting, Denver. **Shuey, RT,** 1985. A simplification of the Zoeppritz's equations. Geophysics, **50**, 609–614; **Smith, GC, and Gidlow PM**, 1987, Weighted stacking for rock property estimation and detection of gas: Geophysical Prospecting, **35**, 993–1014; **Wang,Y**, 1999, Simultaneous inversion for model geometry and elastic parameters, Geophysics, **64**, Pages:182-190. **Wang, Y**, 1999. Approximations to the Zoeppritz's equations and their use in AVO analysis. Geophysics, **64**, 1920-1927; **Zoeppritz K**, 1919, Erdbebenwellen VIII B. On the reflection and penetration of seismic waves through unstable layers. Goettinger Nachr., 66-84.